FISEVIER

Contents lists available at ScienceDirect

# International Journal of Solids and Structures

journal homepage: www.elsevier.com/locate/ijsolstr



# A numerical study on striped lithiation of tin oxide anodes



Ajaykrishna Ramasubramanian<sup>a</sup>, Vitaliy Yurkiv<sup>a</sup>, Anmin Nie<sup>b</sup>, Ali Najafi<sup>c</sup>, Ali Khounsary<sup>a,d</sup>, Reza Shahbazian–Yassar<sup>a</sup>, Farzad Mashayek<sup>a,\*</sup>

- <sup>a</sup> Department of Mechanical and Industrial Engineering, University of Illinois at Chicago, Chicago, IL 60607, USA
- <sup>b</sup> Materials Genome Institute, Shanghai University, Shanghai 200444, China
- <sup>c</sup> Ansys. Inc, Energy Center of Excellence, Houston, TX 77094, USA
- <sup>d</sup> Department of Physics, Illinois Institute of Technology, Chicago, IL 60616, USA

### ARTICLE INFO

#### Article history: Received 21 March 2018 Revised 18 September 2018 Available online 25 September 2018

Keywords: Lithium-ion battery Modeling and simulation Elasto-plastic deformation Striped lithiation Tin oxide

## ABSTRACT

High energy storage capacity of tin oxide (SnO<sub>2</sub>) makes it a promising anode material for high capacity lithium (Li)-ion batteries. Previous experiments reported by Nie et al. (2013) and Huang et al. (2010) have shown that SnO<sub>2</sub> lithiation occurs in two stages. First, Li diffuses rapidly through distinct narrow stripes along the electrode axis. This is followed by a second stage where the diffusion/amorphization of the nanowire occurs. In order to understand and possibly predict this complex chemo-mechanical phenomenon, a finite element (FE) model is developed in this work. The model captures the formation of the striped diffusion regime and the corresponding expansion of the nanowire during the lithiation of SnO<sub>2</sub>. The effect of the stress on the Li diffusion is modeled at the macroscopic level by implementing a stress-dependent expression for the diffusion coefficient. The modeling results clearly show the formation of the striped diffusion regime due to the induced stresses, at low concentrations of Li. This results in a small strain of 0.017 within the nanowire followed by a bulk diffusion and expansion at higher Li concentrations. Thus, the model allows for the spatiotemporally resolved analysis of Li diffusion/intercalation and helps predicting its influence on the mechanical performance of the electrode under the realistic operational conditions.

Published by Elsevier Ltd.

## 1. Introduction

Advanced energy storage systems are of critical importance for a wide range of applications from portable electronics to electric vehicles (Huggins, 2009; Lu et al., 2013; Tarascon and Armand, 2001; Whittingham, 2008). In this regard, lithium (Li) ion batteries (LIBs), based upon graphite electrode, are currently the best performing option. However, the ever-growing demand for higher storage capacity is limiting more widespread applications of the LIBs. The identification of suitable alternative anode materials is a major technological challenge. Tin (Sn) based compounds represent a promising category of materials that can be used as the anode of LIBs, since its maximal theoretical energy density is more than twice that of graphite (Park et al., 2010; Pedersen et al., 2015). The interest in Sn-based systems was triggered by the work of Idota et al. (1997), which uses an amorphous tin composite oxide anode. Many other research groups have since investigated similar compounds and other potential anode materials in the context of LIBs (Courtney, 1997; Di Leo et al., 2015; Ebner et al., 2013; Li et al., 2016; Sandu et al., 2004). However, a commercially viable solution remains to be determined, as there are still major issues that need to be addressed. For example, the large volume expansion that takes place during the lithiation of SnO<sub>2</sub> leads to harmful mechanical processes, which cause fast capacity fading (Guan et al., 2014; Simon and Goswami, 2011). This calls for a better understanding of the lithium insertion into these anode materials.

The *in-situ* transmission electron microscopy (TEM) studies (Chon et al., 2011; Idota et al., 1997; Kepler et al., 1999; Nie et al., 2013) on the lithiation process of SnO<sub>2</sub> nanowire have revealed the morphology evolution and structural changes during the reaction. However, the atomistic mechanisms of dynamical lithiation, at either the early or the final stages of lithiation, in SnO<sub>2</sub> nanowires remain unclear. The experimental work on Sn-based systems by Zhong et al. (2011) reported a peculiarity in Li diffusion and propagation in SnO<sub>2</sub>, which results in a striped diffusion regime. This was further investigated by Nie et al. (2013), which confirmed that Li diffuses at low concentration along stripes (Fig. 1) leading to formation of lithium oxide (Li<sub>2</sub>O) when the SnO<sub>2</sub> nanowire is attached to the Li source. Nie et al. (2013) also reported that the movement, reaction, and generation of mixed dis-

<sup>\*</sup> Corresponding author. E-mail address: mashayek@uic.edu (F. Mashayek).

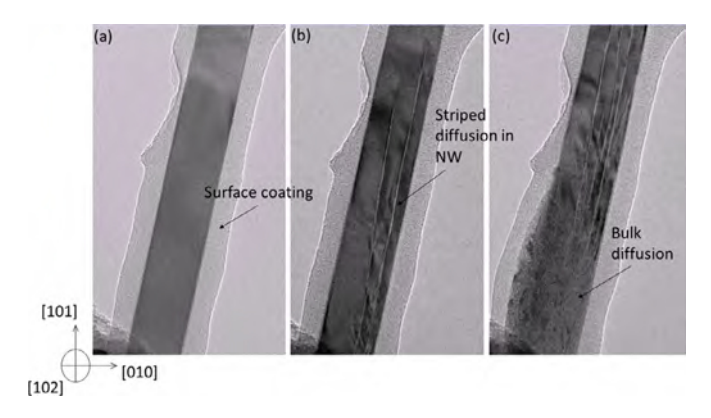


**Fig. 1.** TEM image of lithiation in  $SnO_2$  nanowire (NW), clearly showing the formation of striped diffusion regime followed by bulk diffusion with minimal contrast change on the surface of the NW. (a) The presence of surface carbon coating on pristine  $SnO_2$ , (b) the initial diffusion through the striped region (long-range pipe diffusion) and (c) lithium diffusing through the bulk of the NW (short-range diffusion).

locations leading the lithiated stripes effectively facilitated Li-ion insertion into the crystalline interior. Although the multiple-stripe mechanism was experimentally reported during the lithiation of the SnO<sub>2</sub> nanowires (Zhong et al., 2011), the reason for formation of these stripes are yet to be fully understood. In this regard, predictive continuum scale models that represent such lithiation processes can greatly facilitate and accelerate the development of new high-performing electrodes.

The findings from Nie et al. (2013) show that the lithiation reaction front propagates by long-range Li ion diffusion followed by short-range lithiation of the surrounding matrix. The long-range lithiation process is mediated by the nucleation of dislocations. These dislocation lines can act as fast paths for diffusing atoms, and this elemental phenomenon is known as pipe diffusion (Legros et al., 2008). It is also believed that the lithiation-induced dislocation cores, that are governed by the activation energies through hydrostatic stresses, may act as diffusion channels resulting in pipe diffusion into the SnO<sub>2</sub> crystalline interior thus forming striped diffusion.

Based on the previous findings, in the present work, we develop a model that accounts for the striped diffusion regime due to the uneven contact stress on the surface of the nanowire where it is exposed to the source of Li. In the location where the surface stress is locally large, the stress creates a slip along the longitudinal direction and initiates the stripe formation. We report the results from numerical simulations and qualitatively compare them to the results from the literature to investigate the structural evolution during the lithiation of pristine SnO<sub>2</sub>. This model allows to have a quantitative estimate of the sensitivity of stripe formation and possible shielding effects, interaction and coalescence of the stripes.

The rest of this paper is structured into three parts. Section 2 presents and explains the mathematical formulation and the associated numerical procedure for the developed model. Section 3 presents the numerical results for a striped diffusion structure with a sharp two-phase boundary during lithiation. In this section, the results are compared to the published experimental results (Huang et al., 2010; Nie et al., 2013) for validation. A brief study is conducted to analyze the effect of the distance between the stripes and the effect of change in a few key parameters. The summary and concluding remarks are provided in Section 4.

### 2. Modeling approach and simulation methodology

#### 2.1. Modeling hypothesis

The present modeling framework is developed to reproduce the ions intercalation and the resulting mechanical changes in the  $SnO_2$  electrodes. Based on the hypothesis in the present work, as shown schematically in Fig. 2, when the nanowire is exposed to the Li source, the locally-high contact stress due to the local surface defects on the surface of the nanowire results in a faster diffusion in the longitudinal direction and initiates the stripe formation. Then, as a consequence of the diffusion of lithium along these stripes, high levels of stress are induced. This stress further drives the faster diffusion in the same direction. In order to capture this phenomenon and validate the hypothesis, a FE model is developed, which takes into account the effect of the initial contact stress on diffusion.

Note that in this work, the surface diffusion was considered to be negligible in comparison to the bulk diffusion due to the surface carbon shell coating on the SnO<sub>2</sub> nanowires that were tested. However, in general, the lithiation controlled by surface diffusion can be compatible with the striped lithiation. The lithiation associated with surface diffusion may play an important role in controlling the stress evolution, and future computational studies should consider this effect.

### 2.2. Mathematical modeling and numerical implementation

This section describes the FE model, which numerically implements both the diffusion model and the elastic-plastic model for the lithiation of the SnO<sub>2</sub> nanowire that serves as the anode. The Li concentration and stress-strain fields are solved with an implicit, coupled temperature-displacement procedure. The developed FE model uses a commercial software package, ANSYS (© ANSYS, 2014), as a platform at the continuum level to solve the fully coupled large deformation and mass diffusion problem.

In the current model, we consider the effect of the internal stress field on the activation energy of diffusion, as follows. At the atomic scale, diffusion of a solute particle in a crystal lattice is described as a sequence of movements from one interstitial site to an adjacent site, during which the diffusing particle must overcome the energy barrier caused by its interactions with the surrounding host atoms. Many atomistic and quantum mechanical simulations have shown that this energy barrier is strongly affected by the internal stresses acting on the neighboring crystal atoms. In most scenarios the directions normal to the diffusion influences the diffusion since the expansion in lateral direction is much larger than the longitudinal direction (Liu et al., 2011; Yang et al., 2014), suggesting a dependence of stresses perpendicular to the direction of diffusion. This effect has been referred to as strain-activated mobility by Aziz et al. (1991). But, in case of SnO2 nanowires the longitudinal expansion is much larger than the lateral directions, suggesting a dependence on the hydrostatic stress.

The concurrent reaction and diffusion processes are simulated in a unified manner by treating the interfacial reaction as a non-linear diffusion across a smeared interfacial domain for numerical convenience, despite the difference in the actual interfacial reaction and bulk diffusion processes (Liu et al., 2011). Therefore, the classical diffusion equation is adopted to describe the Li transport in the entire domain

$$\frac{\partial c_{\text{Li}}}{\partial t} = \nabla \cdot (D(c_{\text{Li}}, \sigma_{\text{ax}}) \nabla c_{\text{Li}}). \tag{1}$$

As outlined in the previous sections, the model has to capture the formation of the striped diffusion regime in the pristine  $SnO_2$  phase. In order to achieve this goal, the Li diffusivity,  $D(c_{Li}, \sigma_h)$ , is assumed to be nonlinearly dependent on the local Li concentration,

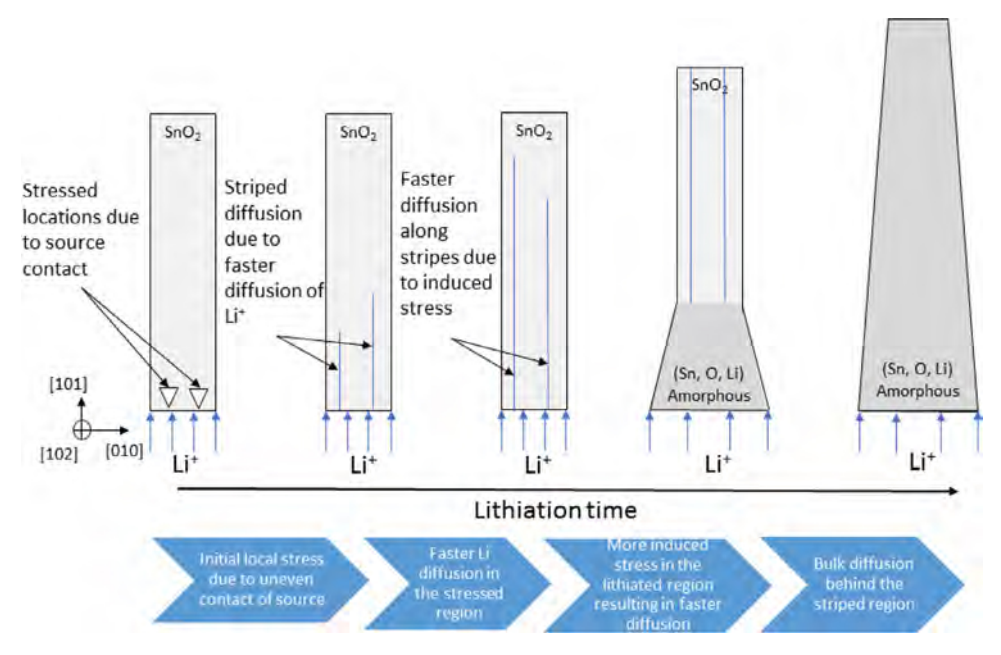


Fig. 2. Schematic of initial and intermediate structures of striped diffusion during simulation. Geometrical changes are not to scale, merely for ilustrative purpose.

 $c_{\rm Li'}$  and the hydrostatic stress,  $\sigma_{\rm h}$ 

$$D(c_{Li}, \sigma_{ax}) = D_{Li}^{0} \left[ \frac{1}{(1 - c_{Li})} - (2\Omega c_{Li}) \right] \cdot \exp\left(-\frac{E^{act}}{RT}\right) \cdot \exp\left(\frac{\kappa V_{m} \sigma_{h}}{RT}\right), \tag{2}$$

where  $D_{ij}^0$  is the pre-exponential factor;  $\Omega$  is a parameter used to control the sharpness of the concentration profile near the reaction front;  $\kappa$  is a positive nondimensional factor, which takes into account the interaction between Li and SnO<sub>2</sub>; V<sub>m</sub> is the molar volume of SnO<sub>2</sub>; R is the universal gas constant and T denotes the temperature. For numerical stability, the maximum of  $D(c_{Li}, \sigma_h)$  is capped at  $10^4 D_{ii}^0$ . The pre-exponential factor  $(D_{ii}^0)$  multiplied by the term in square brackets represents concentration dependence. The first exponential term describes the activation energy term as in the standard Arrhenius equation and the second exponential term in Eq. (2), modifies the activation energy based on the hydrostatic stress magnitude and its direction. The particular form of the diffusion coefficient in Eq. (2) can capture the formation of core shell structures and also capture the effect of stress on the structure and is adopted from the work of Haftbaradaran et al. (2011). The derivation and the detailed explanation of Eq. (2) are given in Appendix A.

In diffusion simulations, the Li concentration behind the reaction front could quickly attain maximum concentration, while those ahead of the front remain nearly zero. The sharp reaction front is consistent with experimental observation and provides a basis for further stress analysis. In order to capture the desired form of the diffusion coefficient the *Usermatth* material routine, a user programmable feature (UPF), within ANSYS is utilized. The Fortran source code of *Usermatth* was reprogrammed in order to add the effect of stress to the diffusion coefficient.

Lithiation of c-SnO $_2$  can characteristically result in amorphous alloys and large deformation. It is now well accepted that materials like lithiated Si or Sn undergo material restructuring through plastic flow (Liu et al., 2012), generating unique deformation morphologies (Chen et al., 2014; Kang and Huang, 2010; Kim et al., 2014). The lithiation-induced deformation is expected to be large and well beyond the applicable region of small-strain theory. Thus, a finite strain model is used to approximate the morphological evolution.

In the finite-strain plasticity framework, deformation is characterized by the elastic and plastic strain rates. The total strain,  $\varepsilon$ , value is decomposed into three components

$$d\varepsilon_{ij} = d\varepsilon_{ij}^{\ e} + d\varepsilon_{ij}^{\ p} + d\varepsilon_{ij}^{\ c} \tag{3}$$

where,  $\varepsilon^{\rm e}$ ,  $\varepsilon^{\rm p}$ , and  $\varepsilon^{\rm c}$  are the elastic, plastic, and chemical strains, respectively. In Eq. (3), assuming that the lithiation-induced electrochemical deformation rate is without spin and the electrochemical strain rate,  $d\varepsilon^{\rm c}$  is proportional to the increment of the normalized Li concentration,  $d\varepsilon_{ij}{}^{\rm c} = \beta_{ij} \cdot dc$ , where  $\beta_{ij}$  is the expansion coefficient. One notices that the chemical strain is analogous to the thermal strain in formulation by considering  $\beta_{ij}$  as the coefficient of thermal expansion and c as the temperature. Thus, a concurrent coupled field element that has both temperature and structural degrees of freedom is used to model the diffusion expansion process. The 8-node quadratic coupled field element (PLANE 223) is used to accommodate both the structural and thermal degrees of freedom. The element has eight nodes with three degrees of freedom (two deformations in-plane direction and temperature/concentration) per node.

In order to account for the influence of the crystalline  $\mathrm{SnO}_2$  core on the expansion, the apparent expansion coefficient,  $\beta_{ij}$ , is assumed to be anisotropic. Such anisotropy plays a critical role in the formation of the shape morphology that is seen during the experiments. The expansion equation due to concentration is critical to relate the physics of the diffusion process to deformation. Then, the stress evolution is captured using appropriate constitutive equations that relate the strains to the stresses. The equations and constitutive relations for stresses are given in Chen et al. (2014) and Liu et al. (2011). In order to accommodate the large deformations, the NLGEOM feature is turned on during the simulation.

#### 2.3. Parametrization

A 2D rectangular shaped strip of tin oxide is simulated in this work to avoid 3D complications. The computational domain and the associated boundary conditions are shown in Fig. 3. The dimensions of the 2D rectangular geometry are of 150 nm  $\times$  5  $\mu$ m.

The appropriate scales for length, time and concentration are chosen to non-dimensionalize the governing equations. The initial

 Table 1

 Simulation parameters with their dimensional and normalized values.

Parameter	Dimensional value	Normalized value	Reference
Lithium concentration, c <sub>Li</sub> SnO <sub>2</sub> nanowire length	$0-3.125 \times 10^5 \text{ mol m}^{-3}$ 150 nm	0-1 1	Zhang et al. (2011)
Young's modulus Yield stress Expansion coefficient $\Omega$ $\kappa$ $D_{L}^{0}$ $E^{\rm act}$	200 GPa (min conc.)-80 GPa (max conc.) 4.9 GPa 0.6 (axial direction)0.45 (longitudinal) 1.46 0.38 9.67·10 <sup>-8</sup> m <sup>2</sup> s <sup>-1</sup> 0.4 eV	218 (min conc.)–88 (max conc.) 5.422 0.6 (axial direction)0.45 (longitudinal)	Zhang et al. (2011) Zhang et al. (2011) Zhang et al. (2011) This work Haftbaradaran et al. (2011) Huang et al. (2010) Huang et al. (2010)

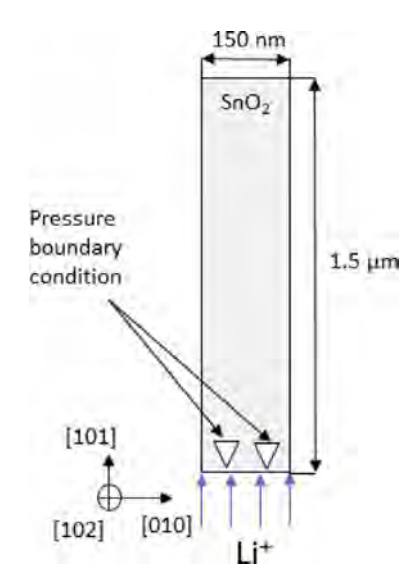


**Fig. 3.** Schematic representation of the 2D rectangular computational domain, together with the main processes and assumptions.

length of the bottom edge of the nanowire (150 nm), as shown in Fig. 3, is taken as the length scale (1) and the time is normalized using the diffusion time,  $t_{\rm d}=l^2/D_{\rm Li}^0$ . The pre-exponential factor  $(D_{ij}^0)$  and the activation energy  $(E^{act})$  for the Li diffusion in  $SnO_2$  are taken from Huang et al. (2010) and are 9.67·10<sup>-8</sup> m<sup>2</sup> s<sup>-1</sup> and 0.4 eV, respectively. The concentration is normalized using the maximum theoretical concentration ( $c_{\mathrm{Li}}^{\mathrm{max}}$ ) which corresponds to the concentration of Li<sub>4.4</sub>Sn. As it is theoretically reported, Li<sub>x</sub>Sn phase expands to 300% the original size (Guan et al., 2014; Simon and Goswami, 2011) in volume comparing to the unlithiated structure; thus, the chemical expansion coefficient,  $\beta$ , is set to 60% and 45% in axial and longitudinal directions, respectively (Zhang et al., 2011). The elastic part of our constitutive model accounts for the Li concentration-dependent Young's modulus and Poisson's ratio. Both Young's modulus and Poisson's ratio are assumed linearly dependent on lithium concentration ranging from 200 GPa and 0.27 at zero concentration of lithium to 80 GPa and 0.24 at maximum lithium concentration, respectively. We adopted the value of 4.9 GPa (Zhang et al., 2011) for yield strength and a hardening modulus of 1 MPa to capture the plastic flow. All the elasto-plastic constants (Young's modulus, Poisson's ratio, yield strength, strain hardness) are normalized by  $c_{ij}^{max}RT$ , which is equal to 1.1 GPa at room temperature and their values are given in Table 1.

The value of dimensionless parameter,  $\Omega$ , which controls the sharpness of the reaction front by controlling the slope of the increase in diffusivity, is kept at 1.46. For values of  $\Omega$ , between 1.46 and 2, the sharpness of the reaction front starts to decrease. For values greater than 2, the diffusivity coefficient turns negative within the operating concentration limits, which is not physi-

cal. The value of  $\kappa$ , which amplifies the diffusion coefficient based on the hydrostatic stress, is taken as 0.38. This value is chosen in such a way that the diffusion coefficient becomes two orders of magnitude higher in the stress region than in the bulk. It should be noted that a similar value of  $\kappa$  was previously reported (Haftbaradaran et al., 2011). Haftbaradaran et al. (2011) have reported that the value of  $\kappa$  could be dependent on the stress sign, such that a tensile stress decreases  $\kappa$ , while a compressive stress increases it. However, the  $\kappa$  dependency on the stress sign was observed for the stress value range between -20 GPa and 12 GPa, thus considering stress range obtained in the present study (-0.1 and 0.1) we assume constant  $\kappa$ . During the finite element simulation, the normalized computational time step size is initially set to  $10^{-6}$ , which is 24.5  $\mu$ s in actual time and is set to be adaptive.

A constant maximum normalized concentration of 1 is applied on the bottom edge of the nanowire, where the source is attached, and the lithium is allowed to diffuse through the inner core. As shown in Fig. 2, a constant pressure load of 0.5 MPa is also applied on the edge where the source is more firmly attached to the surface at two different regions of 5 nm each. These two regions are at a distance  $L\!=\!75\,\mathrm{nm}$  apart. The nanowire is fixed at the geometrical center of the domain to maintain the static equilibrium in translational degrees of freedom.

### 3. Results and discussions

In this section, first the validation of the model's hypothesis is realized by comparison of the model's predictions with the previously published experimental data by Huang et al. (2010) and Nie et al. (2013). A detailed sensitivity study is also presented at the end of this section.

## 3.1. Model validation

We first performed calculations of the diffusion and expansion of the SnO2 nanowire and compared our findings with the results reported by Huang et al. (2010). It should be emphasized that we did not simulate the exact experimental conditions since they are not available in details that are needed to set up the problem. The comparison provided here is therefore qualitative. The representative SnO<sub>2</sub> concentration contours, obtained during the simulation are as shown in Fig. 4. Both the progress of the lithiation process and the evolution of the sharp boundary are shown for different times. For the times of 5 s, 350 s, 550 s and 950 s, we compare the predicted Li concentration with the previously published data. It is noted that these five times correspond to 0%, 10%, 40% and 90% of the progress in lithiation front, thus forming a comprehensive picture of the lithiation phenomenon of the SnO2 nanowire. A good quantitative agreement is obtained between our simulation and the results published by Huang et al. (2010), over the complete investigated time range. The error in lithiation time through the bulk of the nanowire is estimated to be close to 4%. The formation of striped diffusion regime can be clearly seen in this figure.

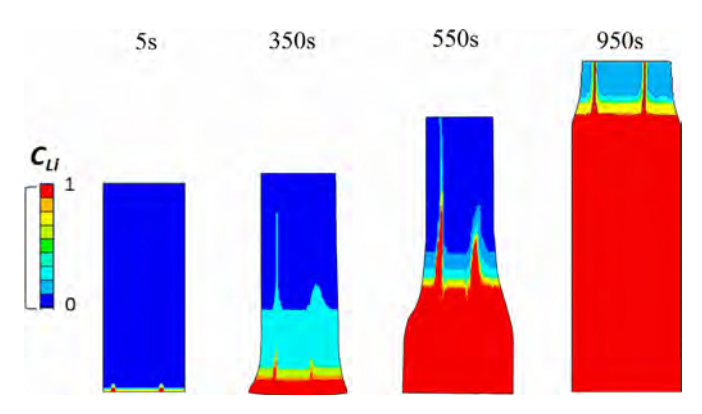


**Fig. 4.** Simulation results showing concentration profile of Li diffusion along the SnO<sub>2</sub> nanowire for times 5 s. 350 s. 550 s and 950 s.

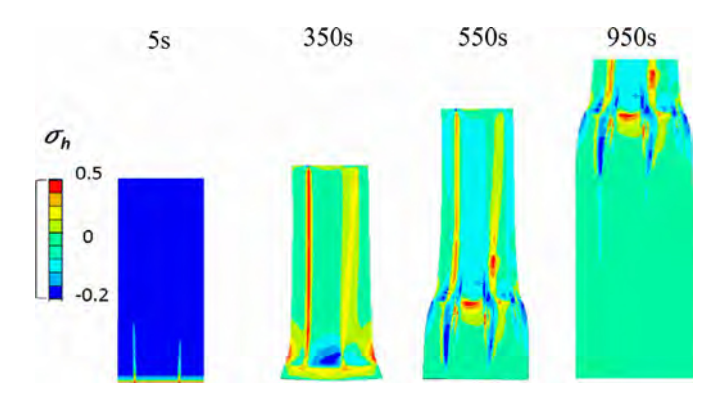


**Fig. 5.** Stress evolution during lithiation of  $SnO_2$  for 0%, 10%, 40% and 90% lithiation (times 5 s, 350 s, 550 s and 950 s). The values of stress are normalized using Young's modulus of elasticity.

In later discussions in this section, the structural changes and the corresponding stresses are discussed. The stripes are initiated at the points where there is an initial stress defined at the surface of the nanowire. The initial stress facilitates faster diffusion only in that region, which subsequently induces more stress. The induced stress leads to enhanced diffusivity and drives the diffusion further in the same direction, resulting in the formation of stripes. From the results, it can be seen that there is a slight shift from a straight-line path of diffusion. This is due to the shift in the direction of the induced stresses as lithiation progresses in each stripe. In a later part of this study, the effect of the distance between the stripes on the induced stress build up is analyzed. From Fig. 4, it can be clearly seen that multiple-stripe formation process is rather quick. Clear stripe formation starts to occur at around 5 s and the thickness of stripes increases with progression of the lithiation. Also from Figs. 4 and 5 we can infer that, since the stripe on the left is formed closer to the wall than the stripe on the right it allows for the formation of the stripe to be relatively faster than the stripe on the right-hand side.

In order to shed more lights on the actual influence of lithiation on stresses, the hydrostatic stress contours are plotted in Fig. 5. From the stress contour, it is evident that the initial stress on the surface induces faster lithiation through a narrow channel, which further induces more stress due to the expansion in these lithiated regions. This induced stress further drives the lithium front to move through these channels.

The equivalent plastic strain contour at the lithiation time of 350 s is shown in Fig. 6, highlighting the bottom part, where the main strain development is observed. As can be seen in Fig. 6, closer to the tip of the striped region, the strain is close to 0.0177 while it remains almost zero in other parts of the nanowire, which

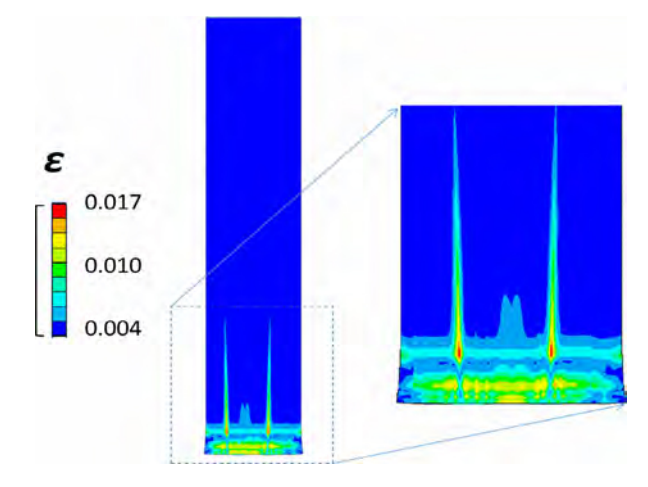


**Fig. 6.** The simulated strain development at the time of 350 s. The zoom-in insertion further highlights the bottom part of the nanowire shown in the left.

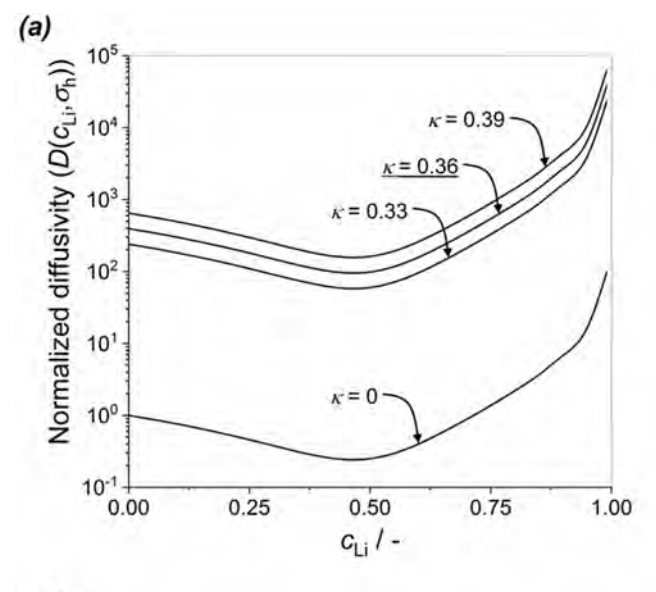
have not been lithiated yet. The results show a good quantitative agreement, with a maximum deviation of 4%, to the previously published TEM results by Nie et al. (2013), thereby supporting our hypothesis that these striped diffusion regimes form due to the effect of the initial contact stresses.

To summarize, the initial lithiation process can be interpreted as follows: Lithiation is initiated at some surface defects or stressed zones and continues along [101] direction. The lithiation induced stress leads to formation of dislocations along the stripes, which further facilitates lithium diffusion into the interior of the nanowire.

## 3.2. Effect of $\kappa$ on diffusion coefficient

The parameter  $\kappa$ , in Eq. (2), plays a crucial role in the evaluation of the diffusion coefficient. As mentioned above, the product  $\kappa V_m \sigma_h$  changes activation energy of Li diffusion in SnO<sub>2</sub>, which reflects the amplification or reduction of the diffusion coefficient. Depending on the magnitude of the stress, parameter  $\kappa$  amplifies the diffusion coefficient in the case of the tensile stress or reduces the diffusion coefficient for the compressive stress. To understand the sensitivity of the diffusion coefficient to  $\kappa$ , the diffusion coefficient is computed for different values of  $\kappa$  as shown in Fig. 7(a). Here,  $\kappa$  is first set to zero to capture the change in the diffusivity with no influence of stress (concentration dependency only). The concentration dependency on the diffusivity, as shown in Eq. (1), reduces the diffusivity to a minimum value at a concentration of  $c_{1i} = 0.45$ . To further analyze and understand the dependency of stress on the diffusivity coefficient a surface plot for the diffusivity coefficient, for the entire range of stress in the domain, is generated as shown in Fig. 7(b). The result clearly indicates that the value of the diffusivity increases by almost two orders of magnitude for a value between the minimum and maximum values of stress. This results in faster ion diffusion that corresponds to the experimental observation by Huang et al. (2010).

To quantify the effect of  $\kappa$  on the formation of stripes, simulations were carried out for three different values of  $\kappa$ , starting from zero, which is equivalent to no effect of stress on diffusion. The concentration contours are plotted for the scenarios where  $\kappa=0$ ,  $\kappa=0.33$  and  $\kappa=0.36$  at a time period of 550 s in Fig. 8. Based on the results shown in Fig. 8, we could see that the rate at which the diffusion happens through the stripes and the diffusion in the bulk changes close to 1% though the change in the value of  $\kappa$  is up to 10%. Also looking at Fig. 7(a), it can be seen that the change in value of  $\kappa$  by 10% increases the diffusivity coefficient by much less than an order of magnitude. When the value of  $\kappa$  is zero there is



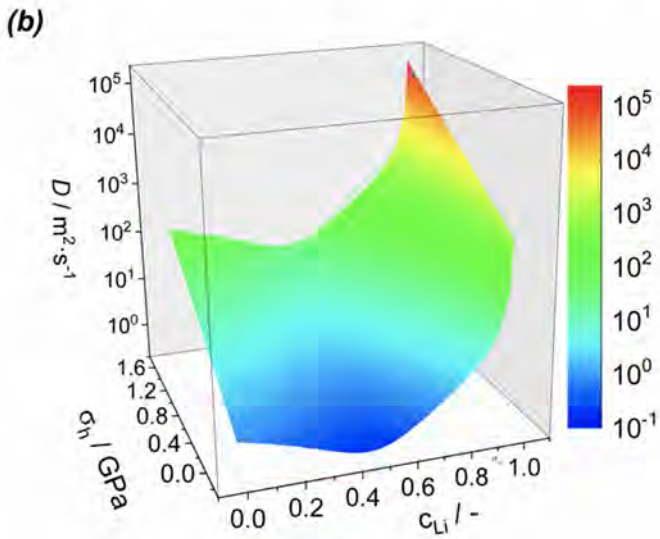


**Fig. 7.** (a) Variation of the diffusivity with concentration for different values of parameter  $\kappa$ . The underlined value of  $\kappa$  is used in this work. (b) Variation of diffusivity with concentration and hydrostatic stress for  $\kappa=0.36$ .

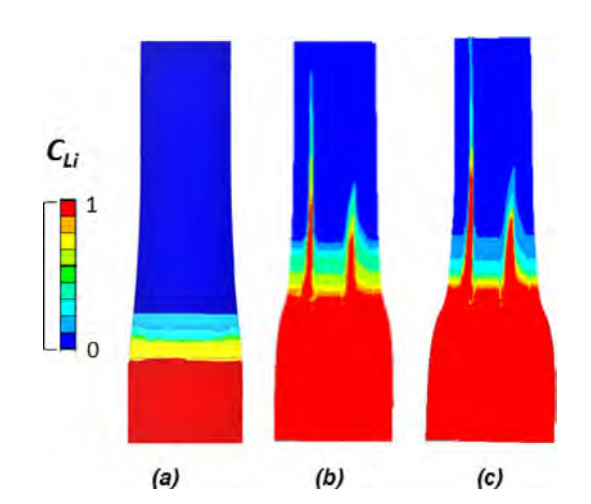


**Fig. 8..** Concentration contours at 550s for different values of  $\kappa$ : (a)  $\kappa=0$  (b)  $\kappa=0.33$  (c)  $\kappa=0.36$ .

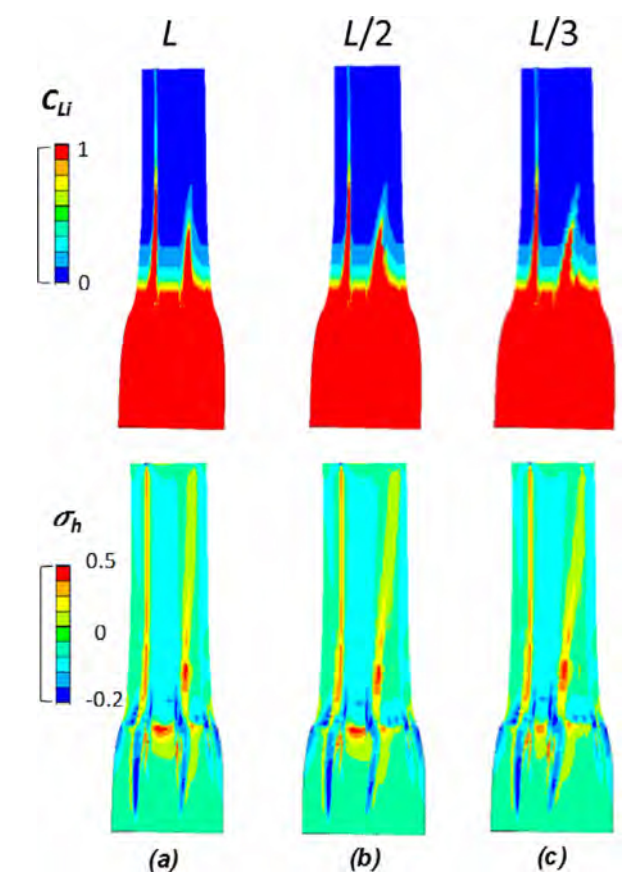


**Fig. 9.** Simulation results showing concentration (top panel) and hydrostatic stress (bottom panel) contours of Li diffusion along the  $SnO_2$  nanowire at  $t=550\,s$  for initial distances between stressed points (a)  $75\,nm$  (b)  $37.5\,nm$  and (c)  $25\,nm$ . The values of stress are normalized using Young's modulus of elasticity.

no effect of stress and thus there is no visible formation of stripes, whereas for the case where  $\kappa=0.33$  the diffusion happens at a much faster rate resulting in clear formation of stripes.

## 3.3. Effect of the distance between the stressed zones

The effect of the distance between the stripes is analyzed by reducing the distance between the initial stressed zones, which drive the formation of the stripes, to half the original value. All parameters described in Table 1 are continued to be used without any changes.

The results from this study, as shown in Fig. 9, reveal that though there is still the formation and propagation of stripes, similarly to those shown in Fig. 2, there are clear differences. Due to the increase in the build-up of compressive stresses between the striped regions, as a consequence of the expansion of the material in the striped regions, we can observe that the diffusion regime is slightly altered. This development of compressive stresses diminishes the diffusion of lithium into this region.

From the results in Fig. 9, it could be observed that the stripes deviate away (at an angle close to 4°) from each other when they are initiated at an initial distance of 37.5 mm instead of 75 mm. This is because the compressive stress buildup between the stripes makes it more difficult for the diffusion closer to the original straight line path. This compressive stress occurs due to the expansion in these stripes resulting in the compression of the region around them. It is also observed that the stripe that is closer to the edge of the nanowire stays almost parallel. This happens due

to the lesser compressive stress between the striped region and the edge of the nanowire as the surface or edge is made traction free.

To further analyze and understand the effect of the distance between the initial stressed locations and the effect of the induced stress between the stripes on diffusion, the distance between the stripes is further reduced to 25 nm. Based on the results in Fig. 9, we could see that when the distance between the initial stressed locations is further reduced the stripes diverge further away (close to 5° for 37.5 nm and close to 7° for 25 nm) from each other due to the build up of higher compressive stresses between the stripes.

#### 4. Summary and conclusions

The design of new electrode materials depends greatly on how the lithiation reaction propagates into them. Therefore, understanding the lithiation mechanism is central to improving the performance of electrode materials during the operation of LIBs. The present work develops a new physics-based finite element model to investigate the structural evolution during the lithiation of pristine SnO<sub>2</sub>. The results from the model clearly show formation of striped diffusion regime due to the induced stresses, at low concentrations of Li.

To develop the model, it is hypothesized that the formation of striped regimes during the diffusion of Li in the SnO<sub>2</sub> electrode is due to the local surface defects and localized high contact stresses from the source at the surface of the electrode. The model is developed in the ANSYS Mechanical APDL solver and uses a coupled finite element diffusion and elasto-plastic approach. The results are shown to have a good qualitative agreement with the lithiation time and strain measurements available in the literature. Through the results, it could be understood that the lithiation induced stress leads to formation of dislocations along the stripes, which further facilitates lithium diffusion into the interior of the nanowire validating our hypothesis. The multiple-stripe formation process is rather quick, and the thickness of the stripes increases with the progression of lithiation. Also, the model is tested for the sensitivity of two key parameters and discussed in detail. It could be seen that the rate of formation of the stripes increases with the increase in the value of the parameter  $\kappa$  that controls the effect of stress on the diffusion coefficient. The study further elaborates the effect of distance between the stripes to further elucidate the effect of stress on the diffusion. It is shown that the stripes diverge from each other because of high compressive stress build up when they are initiated closer to each other. The findings of this study thus provide important insight into the physical basis of microstructural evolution, morphological changes, and mechanical degradation in SnO<sub>2</sub> electrodes.

## Acknowledgments

R. Shahbazian-Yassar acknowledges financial support from the National Science Foundation (award DMR-1620901). AR, VY, RSY and FM acknowledge the financial support from the National Science Foundation (award CBET-1805938).

## Appendix A. Diffusion coefficient

The diffusion of Li in  $SnO_2$  is characterized by the activated diffusion coefficients, where the pre-exponential factor  $(D_{\rm Li}^0)$  and the activation energy  $(E^{\rm act})$  are the two parameters used to calculate the diffusion coefficient

$$D = D_{Li}^{0} \exp(-E^{act}/RT). \tag{A1}$$

Experimental data indicate that Li diffusion in  $SnO_2$  is concentration and stress dependent (Nie et al., 2013). Many functional forms for such dependence are possible. In this work, we

follow the commonly accepted approach based upon the regular solution theory (Liu et al., 2011) for the pre-exponential factor and the theory of molecular kinetics transition (Yang, 2015) for stress-dependence for the activation energy. In particular, the concentration dependence of the pre-exponential factor  $(D_{ij}^0)$ is evaluated by taking the second derivative of the regular solution chemical free energy (Liu et al., 2011), which leads to the term  $D_{\text{Li}}^0[1/(1-c_{\text{Li}})-(2\Omega c_{\text{Li}})]$ . Following the work of Haftbaradaran et al. (2011) and Gao et al. (2013), the activation energy is modified by a factor  $\kappa V_{\rm m} \sigma_{\rm h}$ , where the product  $V_{\rm m} \sigma_{\rm h}$ has the activation energy units and  $\kappa$  is a dimensionless parameter reflecting the amplification or reduction of the diffusion coefficient. Normally, a tensile stress acting on the neighboring host atoms leads to a reduction in the activation energy (or energy barrier as denoted by Haftbaradaran et al. (2011)), while a compressive stress increases it. Thus, linearization of the equation around zero stress leads to a positive dimensionless parameter  $\kappa$  and the activation energy is modified by a factor, where the product has the activation energy units. The final form of the diffusion equation used in the present study is

$$D(c_{\text{Li}}, \sigma_{\text{ax}}) = D_{\text{Li}}^{0} \left[ \frac{1}{(1 - c_{\text{Li}})} - (2\Omega c_{\text{Li}}) \right] \cdot \exp\left(-\frac{E^{\text{act}}}{RT}\right) \cdot \exp\left(\frac{\kappa V_{\text{m}} \sigma_{\text{h}}}{RT}\right)$$
(A2)

#### References

© ANSYS, I., 2014. ANSYS [WWW Document]. © ANSYS, Inc.

Aziz, M.J., Sabin, P.C., Lu, G.Q., 1991. The activation strain tensor: nonhydrostatic stress effects on crystal-growth kinetics. Phys. Rev. B 44, 9812–9816. doi:10. 1103/PhysRevB.44.9812.

Chen, L., Fan, F., Hong, L., Chen, J., Ji, Y.Z., Zhang, S., Zhu, T., Chen, L.Q., 2014. A Phase-field model coupled with large elasto-plastic deformation: application to lithiated silicon electrodes. J. Electrochem. Soc. 161, F3164–F3172. doi:10.1149/2. 0171411jes.

Chon, M.J., Sethuraman, V.A., McCormick, A., Srinivasan, V., Guduru, P.R., 2011. Real-time measurement of stress and damage evolution during initial lithiation of crystalline silicon. Phys. Rev. Lett. 107 doi:10.1103/PhysRevLett.107.045503.

Courtney, I.A., 1997. Electrochemical and in situ X-ray diffraction studies of the reaction of lithium with tin oxide composites. J. Electrochem. Soc. 144, 2045. doi:10.1149/1.1837740.

Di Leo, C.V, Rejovitzky, E., Anand, L., 2015. Diffusion-deformation theory for amorphous silicon anodes: the role of plastic deformation on electrochemical performance. Int. J. Solids Struct. 67-68, 283-296. https://doi.org/10.1016/j.ijsolstr. 2015.04.028

Ebner, M., Marone, F., Stampanoni, M., Wood, V., 2013. Visualization and quantification of electrochemical and mechanical degradation in li ion batteries. Science 342, 716–720. doi:10.1126/science.1241882.

Gao, Y.F., Cho, M., Zhou, M., 2013. Mechanical reliability of alloy-based electrode materials for rechargeable Li-ion batteries 27, 1205–1224. doi:10.1007/s12206-013-0401-7.

Guan, C., Wang, X., Zhang, Q., Fan, Z., Zhang, H., Fan, H.J., 2014. Highly stable and reversible lithium storage in SnO<sub>2</sub> nanowires surface coated with a uniform hollow shell by atomic layer deposition. Nano Lett. 14, 4852–4858. doi:10.1021/nl502192p.

Haftbaradaran, H., Song, J., Curtin, W.A., Gao, H., 2011. Continuum and atomistic models of strongly coupled diffusion, stress, and solute concentration. J. Power Sources 196, 361–370. doi:10.1016/j.jpowsour.2010.06.080.

Huang, J.Y., Zhong, L., Wang, C.M., Sullivan, J.P., Xu, W., Zhang, L.Q., Mao, S.X., Hudak, N.S., Liu, X.H., Subramanian, A., Fan, H., Qi, L., Kushima, A., Li, J., 2010. In situ observation of the electrochemical lithiation of a single SnO<sub>2</sub> nanowire electrode. Science 330 1515–1520. doi:10.1126/science.1195628.

Huggins, R.A., 2009. Advanced Batteries: Materials Science Aspects. Springer-Verlag doi:10.1007/978-0-387-76424-5.

Idota, Y., Kubota, T., Matsufuji, A., Maekawa, Y., Miyasaka, T., 1997. Tin-based amorphous oxide: a high capacity lithium-ion-storage material. Science 276 1395–1397. doi:10.1126/science.276.5317.1395.

Kang, M.K., Huang, R., 2010. A variational approach and finite element implementation for swelling of polymeric hydrogels under geometric constraints. J. Appl. Mech. 77, 61004. doi:10.1115/1.4001715.

Kepler, K.D., Vaughey, J.T., Thackeray, M.M., 1999. Li<sub>x</sub>Cu<sub>6</sub>Sn<sub>5</sub> (0<x<13): an intermetallic insertion electrode for rechargeable lithium batteries. Electrochem. Solid-State Lett. 2, 307–309. doi:10.1149/1.1390819.</p>

Kim, W.S., Hwa, Y., Kim, H.C., Choi, J.H., Sohn, H.J., Hong, S.H., 2014.  $SnO_2@Co_3O_4$  hollow nano-spheres for a Li-ion battery anode with extraordinary performance. Nano Res. 7, 1128–1136. doi:10.1007/s12274-014-0475-2.

Legros, M., Dehm, G., Arzt, E., Balk, T.J., 2008. Observation of giant diffusivity along dislocation cores. Science 319 1646–1649, doi:10.1126/science.1151771.

- Li, Y., Zhang, K., Zheng, B., Yang, F., 2016. Effect of local deformation on the coupling between diffusion and stress in lithium-ion battery. Int. J. Solids Struct. 87, 81–89. http://dx.doi.org/10.1016/j.ijsolstr.2016.02.029.
- Liu, X.H., Zheng, H., Zhong, L., Huang, S., Karki, K., Zhang, L.Q., Liu, Y., Kushima, A., Liang, W.T., Wang, J.W., Cho, J.H., Epstein, E., Dayeh, S.A., Picraux, S.T., Zhu, T., Li, J., Sullivan, J.P., Cumings, J., Wang, C., Mao, S.X., Ye, Z.Z., Zhang, S., Huang, J.Y., 2011. Anisotropic swelling and fracture of silicon nanowires during lithiation. Nano Lett. 11, 3312–3318. doi:10.1021/nl201684d.
- Liu, X.H., Zhong, L., Huang, S., Mao, S.X., Zhu, T., Huang, J.Y., 2012. Size-dependent fracture of silicon nanoparticles during lithiation. ACS Nano 6, 1522–1531. doi:10.1021/nn204476h.
- Lu, B., Song, Y., Guo, Z., Zhang, J., 2013. Modeling of progressive delamination in a thin film driven by diffusion-induced stresses. Int. J. Solids Struct. 50, 2495– 2507. http://dx.doi.org/10.1016/j.ijsolstr.2013.04.003.
- Nie, A., Gan, L.Y., Cheng, Y., Asayesh-Ardakani, H., Li, Q., Dong, C., Tao, R., Mashayek, F., Wang, H.T., Schwingenschlgl, U., Klie, R.F., Yassar, R.S., 2013. Atomic-scale observation of lithiation reaction front in nanoscale SnO<sub>2</sub> materials. ACS Nano 7, 6203–6211. doi:10.1021/nn402125e.
- Park, C.-M., Kim, J.-H., Kim, H., Sohn, H.-J., 2010. Li-alloy based anode materials for Li secondary batteries. Chem. Soc. Rev. 39, 3115–3141. doi:10.1039/B919877F.
- Pedersen, A., Khomyakov, P.A., Luisier, M., Technology, I., 2015. The reversible lithiation of SnO: a three-phase process. Phys. Rev. Appl. 4, 034005-1-034005-11. doi:10.1103/PhysRevApplied.4.034005.

- Sandu, I., Brousse, T., Schleich, D.M., Danot, M., 2004. SnO<sub>2</sub> negative electrode for lithium ion cell: in situ Mössbauer investigation of chemical changes upon discharge. J. Solid State Chem. 177, 4332–4340. doi:10.1016/j.jssc.2004.06.032.
- Simon, G.K., Goswami, T., 2011. Improving anodes for lithium ion batteries. Metall. Mater. Trans. A Phys. Metall. Mater. Sci. 42, 231–236. doi:10.1007/s11661-010-0438-5.
- Tarascon, J.M., Armand, M., 2001. Issues and challenges facing rechargeable lithium batteries. Nature 414, 359–367. doi:10.1038/35104644.
- Whittingham, M.S., 2008. Materials challenges facing electrical energy storage. MRS Bull. 33, 411–419. doi:10.1557/mrs2008.82.
- Yang, F., 2015. Field-limited migration of Li-ions in Li-ion battery. ECS Electrochem. Lett. 4, A7–A9. doi:10.1149/2.0071501eel.
- Yang, H., Fan, F., Liang, W., Guo, X., Zhu, T., Zhang, S., 2014. A chemo-mechanical model of lithiation in silicon. J. Mech. Phys. Solids 70, 349–361. doi:10.1016/j. imps.2014.06.004.
- Zhang, L.Q., Liu, X.H., Liu, Y., Huang, S., Zhu, T., Gui, L., Mao, S.X., Ye, Z.Z., Wang, C.M., Sullivan, J.P., Huang, J.Y., 2011. Controlling the lithiation-induced strain and charging rate in nanowire electrodes by coating. ACS Nano 5, 4800–4809. doi:10.1021/nn200770p.
- Zhong, L., Liu, X.H., Wang, G.F., Mao, S.X., Huang, J.Y., 2011. Multiple-stripe lithiation mechanism of individual SnO<sub>2</sub> nanowires in a flooding geometry 248302, 18–21. doi:10.1103/PhysRevLett.106.248302.